Available online at www.sciencedirect.com
ScienceDirect
Journal of the European Ceramic Society 32 (2012) 185–194
www.elsevier.com/locate/jeurceramsoc

Preparation of high solids content nano-titania suspensions to obtain spray-dried nanostructured powders for atmospheric plasma spraying

Mónica Vicent [a,*], Enrique Sánchez [a], Arnaldo Moreno [a], Rodrigo Moreno [b]

[a] *Instituto de Tecnología Cerámica (ITC), Universitat Jaume I (UJI), Castellón, Spain*
[b] *Instituto de Cerámica y Vidrio (ICV), CSIC, Madrid, Spain*

Received 24 March 2011; received in revised form 28 July 2011; accepted 7 August 2011
Available online 25 August 2011

Abstract

Nanosized TiO_2 powder with an average primary size of ~20 nm and surface area of ~50 m^2/g (Aeroxide® P25, Degussa-Evonik, Germany) was used as starting material. A colloidal titania suspension from the same supplier was also used (W740X). The dispersing conditions were studied as a function of pH, dispersant content, and solids loading. Well-dispersed TiO_2 nanosuspensions with solids contents up to 30 vol.% (62 wt%) were obtained by dispersing the powder with 4 wt% PAA. Suspensions with solids contents as high as 35 vol.% were prepared by adding the TiO_2 nanoparticles to the TiO_2 colloidal suspension under optimised dispersing conditions.

TiO_2 powder reconstitution was performed by spray drying both types of nanosuspensions to obtain free-flowing micrometre-sized nanostructured granules. The spray-dried nanostructured TiO_2 granules were deposited on austenitic stainless steel coupons using atmospheric plasma spraying. Coating microstructure and phase composition were characterised using scanning electron microscopy and X-ray diffraction techniques.

Keywords: A. Drying; A. Suspensions; B. Nanocomposites; D. TiO_2; Rheology

1. Introduction

Titania (TiO_2)-based materials are very attractive due to their photocatalytic activity.[1] TiO_2 occurs naturally as minerals with rutile, anatase, and brookite phases. Rutile and anatase phases have been extensively studied and have significant technological uses, principally with relation to their optical properties, since both are transparent in the visible range and absorb in the near-ultraviolet region.

As a photocatalyst, TiO_2 can be used in the form of powder and thin films.[2] There is a growing interest in developing reliable, economical, and environmentally-friendly methods for manufacturing thin and thick coatings and layered systems. Layered ceramics and coatings have drawn increasing attention because of their ability to satisfy critical requirements that are not met by any monolithic material.[3] Current methods for producing these coatings include chemical and physical vapour deposition (CVD and PVD), thermal spraying, self-propagating high-temperature synthesis (SHS), etc.[4,5] Atmospheric plasma spraying (APS), a thermal spraying method, allows finely nanostructured coatings to be fabricated.[6–9]

In a plasma spraying process, a feed material is melted and accelerated until it impacts upon the substrate where it is rapidly cooled, forming the coating. According to the literature, nanostructured coatings could enhance the properties of the final material. In order to obtain nanostructured coatings by plasma spraying, it is convenient to use nanoparticles as raw material. However, nanoparticles are not directly sprayable owing to their small mass. Sprayable micrometre-sized powders made up of nanoparticles, also known as nanostructured powders, can be obtained by granulation[10] or freeze-drying[11] methods, spray drying being the most widely used method.[12,13] Recent studies have focused on the conventional spray-drying process for producing nanoporous/mesoporous spheres – for example, using compositions based on titania,[14,15] silica,[16,17] and other materials.[18]

Though nanostructured powders could provide enhanced properties, their use still remains a challenge, however, owing to the health and hazard risks involved in the direct handling of nanosized powders.[13]

* Corresponding author.
E-mail address: monica.vicent@itc.uji.es (M. Vicent).

0955-2219/$ – see front matter © 2011 Elsevier Ltd. All rights reserved.
doi:10.1016/j.jeurceramsoc.2011.08.007

In order to produce such spray-dried nanostructured powders, homogeneous suspensions of nanoparticles are required. However, most papers on coatings obtained by APS from spray-dried nanostructured powders only note the reconstitution process, without providing any details on the suspension preparation step. Further research on nanosuspension preparation for obtaining reconstituted powders by APS is, therefore, still needed.

The dispersion of micrometre-sized ceramic powders, such as titania, in either an aqueous or a non-aqueous medium has drawn considerable attention.[19,20] Stable slurries with high solids loading and low viscosity are known to be required for spray drying.[21,22] This is difficult to achieve with particles in the nanometre range because the increased surface activity and higher interparticle interactions make it difficult to stabilise the particles in the dispersing medium.[23–25]

This study focuses on the preparation and optimisation of concentrated nanosized titania suspensions for reconstituting appropriate spray-dried nanostructured powders for producing APS coatings. Two different starting commercial raw materials were used: a titania nanopowder and a titania nanoparticle suspension from the same supplier. The effect of suspensions solids loading on the characteristics of the resulting granules and coatings was also examined.

2. Experimental

2.1. Starting raw materials characterisation

A commercial nanopowder (Aeroxide® P25) and a commercial nanoparticle suspension (Aerodisp® W740X), both supplied by Degussa-Evonik (Germany), were used in this study. The main physico-chemical characteristics provided by the suppliers are shown in Tables 1 and 2. According to the supplier, the colloidal suspension was prepared from the same P25-powder, and contained anatase and rutile phases in a ratio of about 3:1.[26] The dry powders were characterised by transmission electron microscopy, TEM (H7100, Hitachi, Japan and CM10, Philips, Netherlands).

Specific surface areas were determined using the single-point BET method (Monosorb, Quantachrome Co., USA). In addition, thermogravimetric analyses TG/DTA (STAY09, Netzsch, Germany) were performed at a heating rate of 0.17 °C/s to ascertain the possible presence of additives or precursors.

2.2. Colloidal behaviour characterisation

The colloidal behaviour of the dry P25 nanopowder in water was reported in a previous study,[27] in which a commercial salt (DURAMAX™ D-3005, Rohm & Haas/Dow Chemicals, USA) of polyacrylic acid-based polyelectrolyte (PAA), with 35 wt% active matter was used.

The colloidal stability of TiO_2 nanopowders was studied in terms of zeta potential as a function of deflocculant content and pH, using a Zetasizer NanoZS instrument (Malvern, UK), based on the laser Doppler velocimetry technique. Suspensions were diluted to a concentration of 0.005 wt% titania, using KCl 0.01 M as inert electrolyte. The pH values were determined with a pH-meter (716 DMS Titrine, Metrohm, Switzerland) and were adjusted with HCl and KOH solutions (0.1 and 0.01 M). To improve the dispersion state an ultrasounds probe (UP 400S, Dr Hielscher GmbH, Germany) was used in order to avoid agglomeration. The diluted aqueous suspensions were also used to determine particle size distribution by dynamic light scattering (DLS) using the same equipment as that used for the zeta potential measurements. In a second phase, the colloidal behaviour of the nanopowder dispersed in the commercial nanosuspension was evaluated in two different pH ranges.

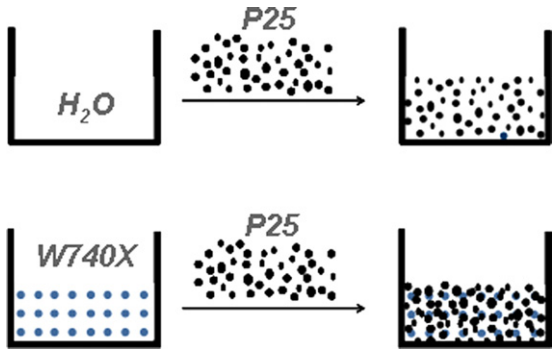

Fig. 1. Processing flow chart of diluted and concentrated nanosuspensions prepared by dispersing the P25-powder in water and in the colloidal W740X-suspension, respectively.

2.3. Rheological study

The rheological behaviour of all the nanosuspensions was determined using a rheometer (Haake RS50, Karlsruhe, Germany) operating at a controlled shear rate (CR). Flow curves were obtained with a three-stage measuring program with a linear increase in the shear rate from 0 to 1000 s^{-1} in 300 s, a plateau at 1000 s^{-1} for 60 s, and a further decrease to zero shear rate in 300 s. The measurements were performed at 25 °C using a double cone and plate system.[28]

Fig. 1 schematically illustrates the procedure used to prepare the two types of suspensions: on the one hand, suspensions were prepared by adding the P25 nanopowder to water (with 4 wt% PAA) and, on the other, suspensions were prepared by dispersing the P25-powder in the commercial colloidal suspension using the same dispersant content. In both cases, low concentration suspensions were prepared by mechanical stirring, but high solids loadings could only be reached by using a sonication probe for dispersion, sonication time changing for each suspension.

2.4. Spray drying

Spray-dried granules were obtained from a diluted (i.e. commercial) suspension at 10 vol.% and from a concentrated suspension (prepared in-house) at 30 vol.% in a spray dryer (Mobile Minor, Gea Niro, Denmark) with a drying capacity of 7 kg water/h.[12,27] Both types of granules were fully characterised before APS deposition. Granule size distribution was measured by laser light scattering (Mastersizer S, Malvern, UK) and density was measured by helium pycnometry (Multipycnometer,

Table 1
Main characteristics of the commercial TiO_2 nanoparticles (Aeroxide® P25), information provided by the supplier.

Average primary particle size (nm)	Specific surface area (m^2/g)	pH in 4% dispersion	Purity (wt%)
21	50 ± 15	3.5–4.5	99.5

Table 2
Main characteristics of the commercial TiO_2 suspension (Aerodisp® W740X), information provided by the supplier.

Suspension type	Solids content (wt%)	pH	Viscosity	Aggregate size	Density (20 °C)
Aqueous	40.0 ± 0.1	5.0–7.0	≤1000 mPa s	≤100 nm	1.41 g/cm^3

Quantachrome Co., USA). Specific surface area and pore structure were measured by nitrogen gas adsorption (TriStar 3000, Micromeritics, USA), though pore structure was also measured by mercury intrusion porosimetry, MIP (AutoPore IV 9500, Micromeritics, USA). A field-emission gun environmental scanning electron microscope, FEG-ESEM (QUANTA 200FEG, FEI Company, USA), equipped with an energy-dispersive X-ray spectrometer (EDAX Genesis) was used to examine the feedstock microstructure. In addition, agglomerate apparent density was calculated from tapped powder density by assuming a theoretical packing factor of 0.6, which is characteristic of monosize, spherical particles.[29] Powder flowability was evaluated in terms of the Hausner ratio, defined as the ratio of the tapped density to the apparent (or poured) density of the powder.[29]

2.5. APS processing

TiO_2 coatings were deposited by an atmospheric plasma spray (APS) system using spray-dried nanostructured granules.[12] The metallic substrates (AISI 304) were grit-blasted with corundum before the plasma spray application in order to clean and roughen the surface. The plasma spray system consisted of a gun (F4-MB, Sulzer Metco, Germany) operated by a robot (IRB 1400, ABB, Switzerland). Deposition was performed using argon as primary and hydrogen as secondary plasma gas. Plasma spray conditions are detailed in Table 3. Finally, the crystalline phases were determined by X-ray diffraction (XRD D8 Advance, Bruker AXS, Germany), microstructure being determined by FEG-ESEM.

3. Results and discussion

3.1. Starting raw materials characterisation

Fig. 2 shows TEM micrographs of the P25-powder and the solid material of the W740X-suspension, in which spherical nanoparticles may be observed. The microstructural observations of both nanopowders showed that the particles were agglomerated and the primary particles were about 30–40 nm in diameter. The W740X-suspension contained P25-nanopowder, as reported by the supplier, though the dispersion in water was presumably obtained with the aid of some processing additives, which might change certain physico-chemical characteristics. The specific surface area of the P25-powder and the W740X-suspension solid fraction was 48.5 and 49.0 m^2/g, respectively.

The results of the thermogravimetric and differential thermal analyses (TG/DTA) performed on the P25-powder and the W740X-suspension solid fraction are presented in Fig. 3. It shows that there were important differences between the two powders. In the P25-powder, a small amount (less than 2.5 wt%) of organic matter was burned out before 500 °C. However, in the W740X-suspension solid fraction, a weight loss of 4.5 wt% was detected, 0.5 wt% of the total weight loss corresponding to humidity. In the W740X-suspension solid fraction, a small peak was detected at 700 °C in the DTA, which could be related to organic matter burnout and/or removal of alkyl groups associated with synthesis precursors.

Table 3
APS parameters.

Ar slpm	H_2 slpm	He slpm	[a]I (A)	[b]d (m)	[c]v (m/s)
38	14	–	600	0.120	1

slpm: standard litre per minute.
[a] Arc intensity.
[b] Spraying distance.
[c] Spraying velocity.

3.2. Colloidal behaviour characterisation

Colloidal behaviour was studied by measuring particle size distribution and zeta potential as a function of sonication time, and pH and deflocculant content of the two suspensions.

The application of ultrasounds (US) plays a key role in nanoparticle dispersion[23] and needs to be optimised in each suspension to assure dispersion without re-agglomeration.[24] Fig. 4 shows the effect of US time on the particle size distribution of the colloidal W740X-suspension and of a suspension prepared from P25-powder, both diluted to a titania concentration of 0.005%. The particle size distribution of the diluted P25 suspensions (Fig. 4a) exhibited a monomodal particle size distribution after 30 s sonication, with a mean particle size of ∼200 nm. However, when 60 or 120 s was applied, a bimodal distribution was observed, in which the first peak appeared at ∼140 and ∼100 nm, respectively, whereas the second peak increased from 300 to 500 nm after 60 or 120 s sonication. That is, sonication broadened the size distribution and increased the volume of the finer fraction, which suggests that new surfaces were being formed and particles tended to re-agglomerate. These measurements indicated that 30 s sonication could be deemed an optimum value for the P25-powder in the diluted suspension. In the case of the

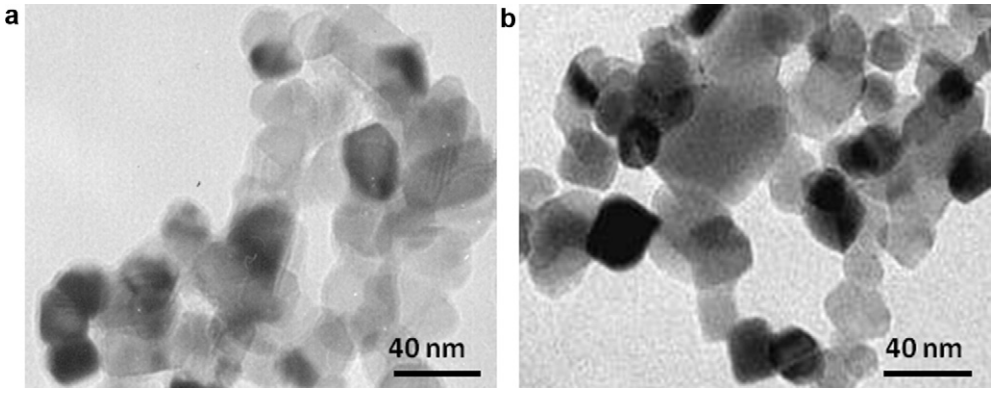

Fig. 2. TEM micrographs of TiO_2: a) P25-powder and b) W740X-suspension solid fraction.

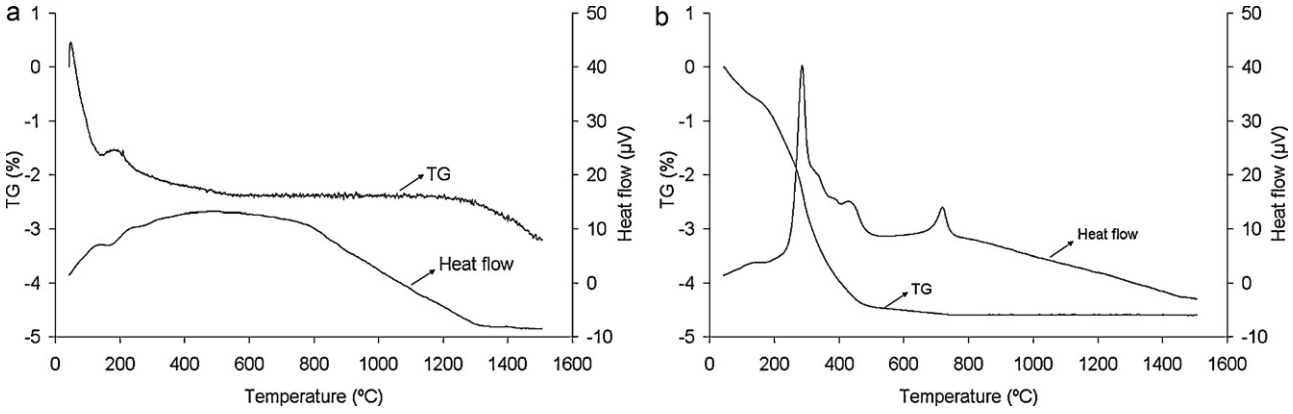

Fig. 3. TG/DTA measurements of a) P25-powder and b) W740X-suspension solid fraction.

W740X sample (Fig. 4b), increasing sonication time from 180 to 480 s encouraged dispersion and decreased agglomerate size from 400 to 150 nm. In contrast, longer sonication time (900 s) produced the opposite effect and increased agglomerate size to 2000 nm.

The evolution of zeta potential with pH of the P25-powder and the W740X-suspension is shown in Fig. 5. Although both powders were nominally the same, the measured isoelectric point (IEP) changed from pH 7 for the P25-powder to pH 6 for the W740X-suspension. This confirmed the assumption noted above that some processing additive had been used as a stabilising agent in the commercial colloidal suspension or that some precursor material was still present. When a polyelectrolyte (PAA) was added as a dispersant, the IEP of the P25-powder shifted from 7.0 to 4.0, 3.8, and 2.7 after the addition of 1.0, 2.0, and 4.0 wt% deflocculant, respectively.[27] This confirmed the successful adsorption of PAA onto the titania nanosized powder.[25] Based on these curves, 4.0 wt% PAA was selected for further experiments as it provided the best zeta potential values (∼−40 mV) in a wider pH range. Higher deflocculant contents were not studied because these suspensions were sufficiently homogeneous.[27]

The evolution of zeta potential with PAA content of the P25-powder and of the W740X-suspension at two different pH values (7 and 10) is shown in Fig. 6. It may be observed that the addition of PAA increased the zeta potential of the P25 suspensions, whereas in the case of the colloidal W740X-suspension the zeta potential remained constant at each studied pH after

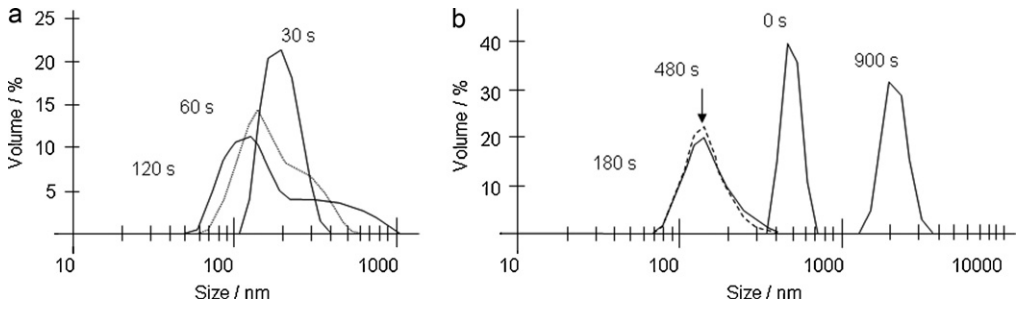

Fig. 4. Particle size distribution of diluted suspensions prepared from a) P25-powder and b) W740X-suspension after sonication.

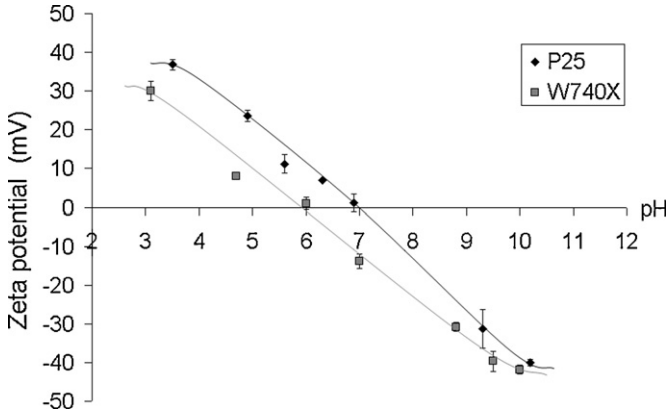

Fig. 5. Evolution of zeta potential with pH of the P25-powder and the W740X-suspension.

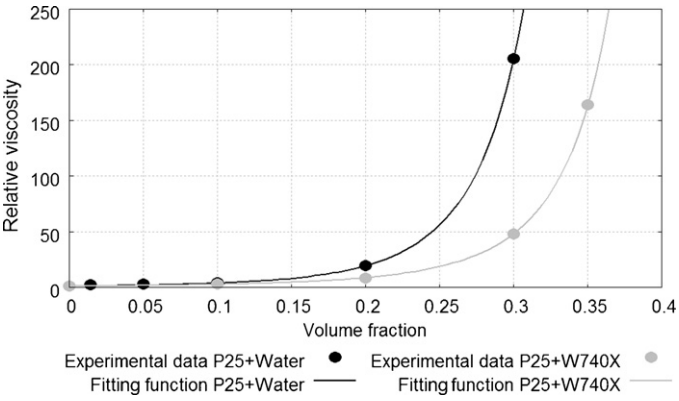

Fig. 8. Fitting of relative viscosity versus solids volume content to the Krieger–Dougherty equation.

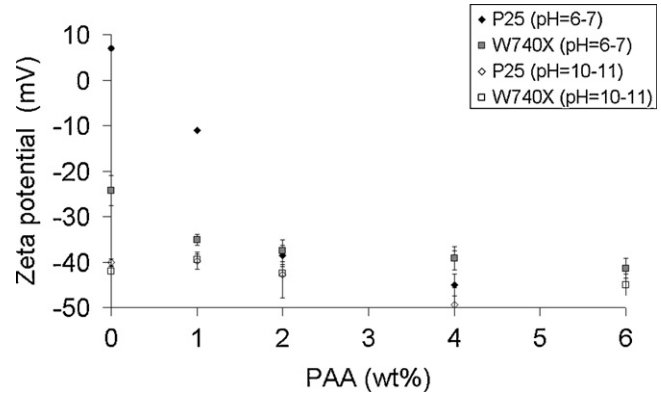

Fig. 6. Effect of the PAA addition on the zeta potential measurements (at two different pH values) using the P25-powder and the W740X-suspension.

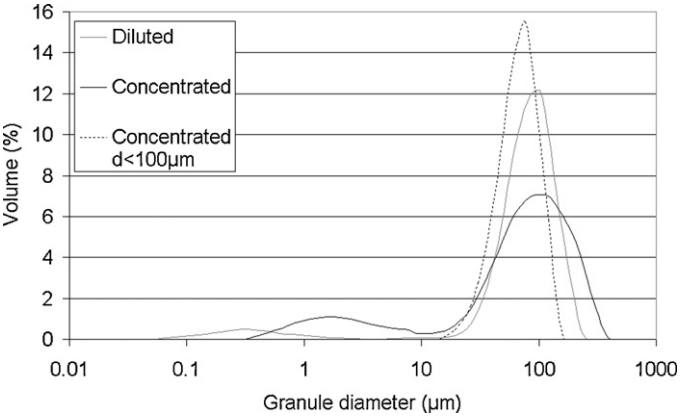

Fig. 9. Granule size distribution of the spray-dried powder obtained from the diluted and the concentrated suspensions. The granule size distribution of the spray-dried powder obtained from the concentrated suspension sieved at 100 μm is also displayed.

the PAA additions. This again suggests that the powder surfaces in the commercial suspension were covered with some additive or precursor that impeded PAA adsorption. The addition of 4.0 wt% PAA provided the P25 suspensions with higher zeta potential values, while it maintained the stability of the commercial W740X suspensions. This PAA content was therefore used for the mixtures.

The particle size distribution measured by DLS in the commercial suspension indicated that the suspension had a mean particle size of 32 nm, demonstrating that appropriate dispersion had been achieved with PAA.

3.3. Rheological study

Titania nanosuspensions of P25-powder in water were prepared at solids loadings of 30 vol.% (~62 wt%) by dispersion

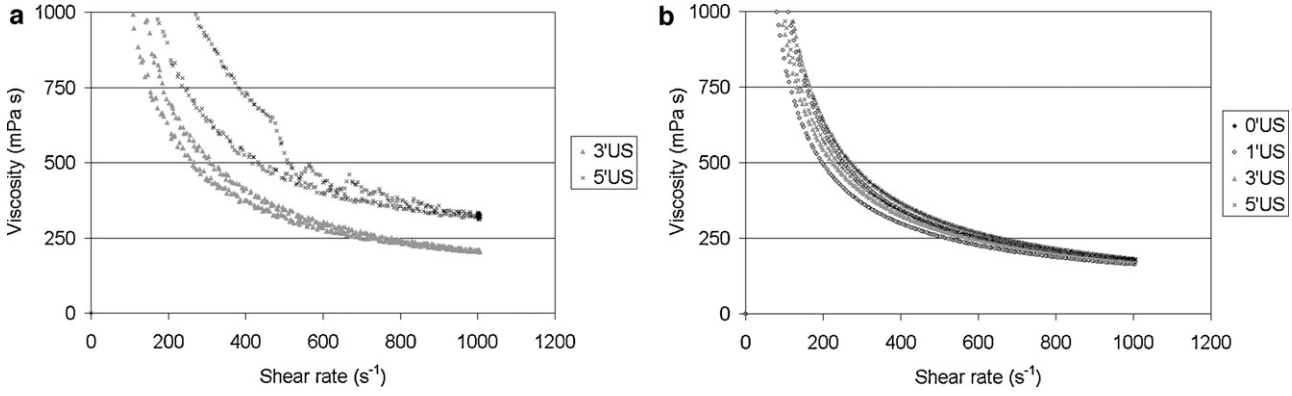

Fig. 7. Viscosity curves of a) 30 vol.% TiO_2, obtained by adding the nanopowder to water (0′ and 1′ US could not be measured) and b) 35 vol.% TiO_2, obtained by adding the nanopowder to the commercial nanosuspension.

Table 4
Main characteristics of the spray-dried nanosuspensions.

Nanosuspension	Solids content (vol.%)	[a] ρ (g/cm^3)	pH	[b] η at 100 s^{-1} (mPa s)	[b] η at 1000 s^{-1} (mPa s)
Diluted	10	1.26	6.7	2.6	2.8
Concentrated	30	1.71	7.4	212	48

[a] Density was measured by a pycnometer.
[b] Viscosity values taken from the upward flow curves.

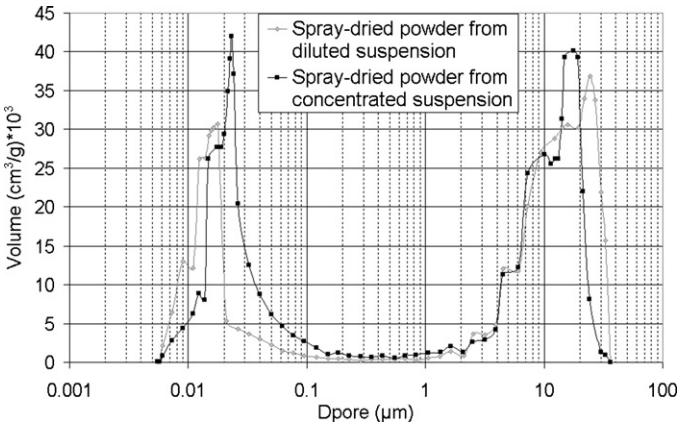

Fig. 10. Pore size distribution of the spray-dried powder obtained from the diluted and the concentrated suspensions measured by mercury intrusion porosimetry.

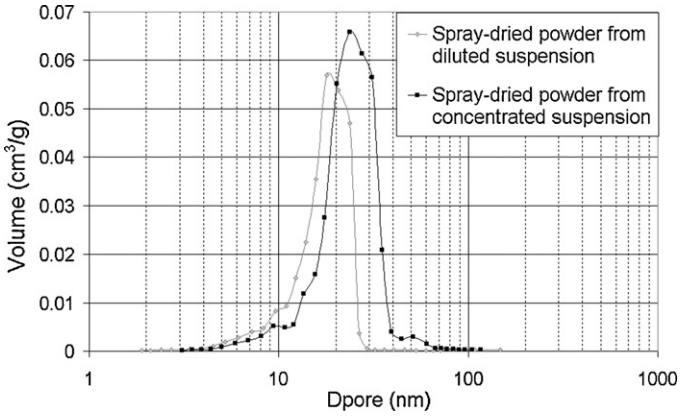

Fig. 11. BJH curves of the spray-dried powder obtained from the diluted and the concentrated suspensions measured in the desorption step.

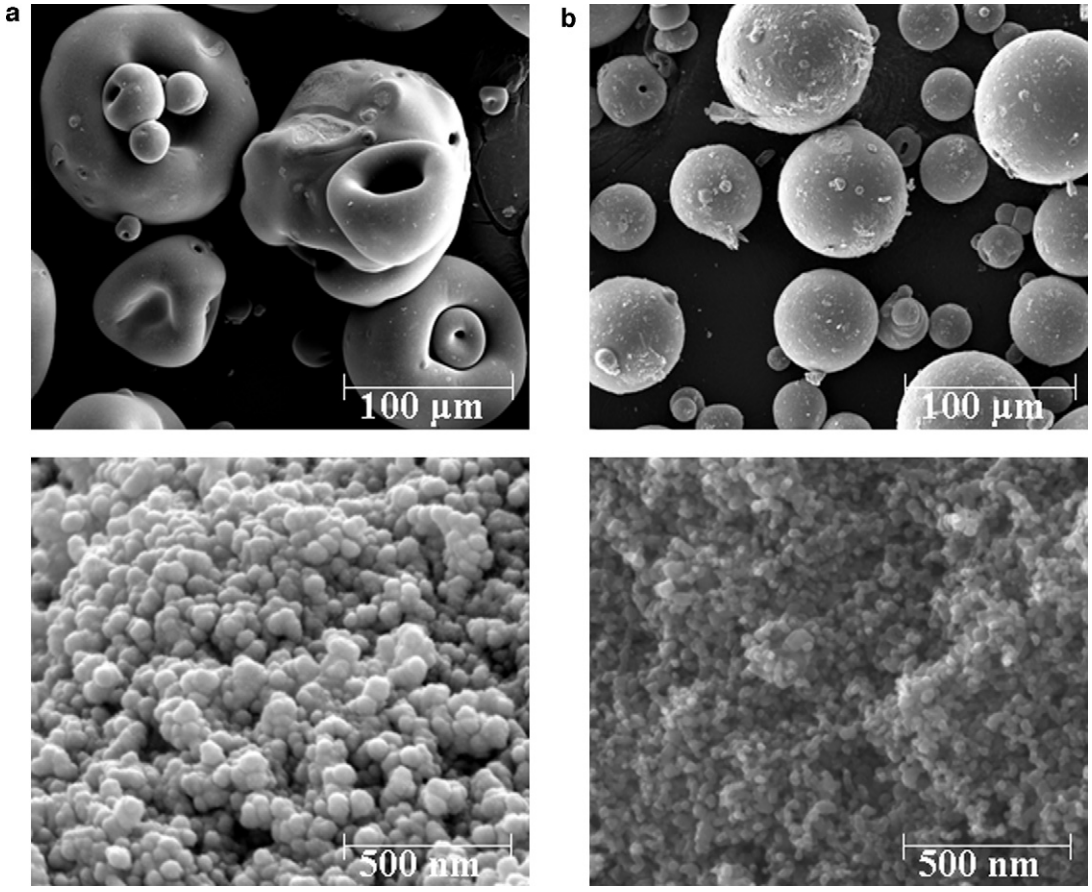

Fig. 12. FEG-ESEM micrographs of granules obtained from a) diluted nanosuspensions and b) concentrated nanosuspensions.

with the sonication probe. Fig. 7a shows the viscosity curves of the P25 suspensions prepared at 30 vol.% solids with sonication times of 3 and 5 min. Suspensions with lower sonication time could not be measured because of their high viscosity.[27]

Suspensions of P25-powder dispersed in the colloidal W740X-nanosuspension were prepared up to solids contents of 35 vol.% (~69 wt%). This route enabled suspensions to be prepared with a higher solids content and lower viscosity than those of the P25-nanosuspensions, as may be observed in Fig. 7b, which shows the viscosity curves of suspensions of P25-powder added to the colloidal W740X-suspension prepared to a total solids content of 35 vol.% at sonication times of 0, 1, 3, and 5 min.

The evolution of relative viscosity with solids volume fraction of the two suspensions (P25-powder + water and P25-powder + W740X-suspension) is depicted in Fig. 8. The viscosity values were all taken from the downward flow curves at a shear rate of 1000 s^{-1}. The experimental points were fitted to the Krieger–Dougherty equation.[30] The figure shows that, in both cases, the experimental data fitted the model quite well. The maximum volume fraction (Φ_m) determined by the model was 0.5 for the two nanosuspensions (in water and in colloidal suspension), because the W740X-suspension solid fraction comprised P25-nanopowder. Intrinsic viscosity [η] decreased from 11.6 in the P25 + water suspension to 8.4 in the suspension obtained from the P25 + W740X sample, indicating higher particle sphericity in the latter (lower agglomeration giving rise to irregular shapes in the former), as expected for the colloidal suspension.

3.4. Characterisation of the spray-dried granules

Two nanosuspensions were prepared (Table 4) for spray drying: the commercial 10 vol.% W740X-nanosuspension and a suspension with a high solids content, 30 vol.% (~62 wt%), obtained by dispersing P25-powder in the commercial W740X-nanosuspension, referred to hereafter as the diluted suspension and the concentrated suspension, respectively. Despite the much higher viscosity of the concentrated suspension, this was also readily spray dried.

Fig. 9 shows the particle size distribution of both types of granules. Due to the high viscosity of the concentrated suspension, large agglomerates (balls) appeared. The resulting spray-dried powder therefore needed to be sieved to avoid transport problems caused by these coarse agglomerates when the granulated powder was fed into the plasma flame torch.

Table 5 details the principal characteristics of the spray-dried granules obtained from the diluted and concentrated nanosuspensions. These include particle size (measured by laser diffraction), real density (measured by helium pycnometry), specific surface area (measured by nitrogen adsorption at 77 K, BET method), two representative pore structure parameters (cumulative volume and mean pore diameter) obtained by nitrogen gas adsorption, and granule mean pore diameter measured by porosimetry.

The pore size distribution measured by MIP (Fig. 10) shows the inter- and intra-granular porosity of the resulting powders.

Table 5
Main characteristics of the spray-dried granules obtained from 10 vol.% (diluted) and 30 vol.% (concentrated) nanosuspensions.

Suspension	Laser diffraction	Helium pycnometry	N_2 adsorption/desorption isotherm			Mean pore size (μm)		Powder flowability	
	$D_{v,0.5}$ (μm)	Real density (kg/m^3)	Surface area (m^2/g)	Accumulative volume in desorption curve (cm^3/g)	$D_{pore\ 4V/A}$ (nm)	Inter-granule	Intra-granule	Hausner ratio	Density (kg/m^3)
Diluted	76	3600	51	0.272	15.3	18.2	0.02	1.20	1870
Concentrated	63	3400	50	0.355	21.0	14.9	0.02	1.17	1620

The pore size distribution measured by nitrogen gas adsorption, Barret–Joyner–Halenda (BJH) method (Fig. 11), only exhibits the intra-granular porosity.

The inter-granular mean pore diameter (Table 5) of the granules obtained from the diluted and from the concentrated suspensions was quite similar. The FEG-ESEM observations (Fig. 12 top) revealed that the granules obtained from the concentrated suspension were highly spherical and uniform, whereas the agglomerates from the diluted suspension displayed an irregular doughnut-shaped geometry. This greater heterogeneity may be attributed to liquid-phase separation during the spray-drying operation, possibly due to some surface tension modifier incorporated into the commercial suspension.[12] The irregular granules resulting from the diluted suspension therefore yielded poorer layer packing, and the inter-granular mean pore diameter of these granules was larger.

At higher magnifications (Fig. 12 bottom), the micrographs show that both granules were built up of adhering nanoparticles, indicating that the granules were porous (intra-granular porosity) and consisted of an agglomeration of primary nanoparticles. The intra-granular mean pore diameter measured by BJH was more accurate than that measured by MIP. With regard to this kind of porosity, the mean pore size of granules (Table 5) obtained from the diluted suspension was lower than that of the granules resulting from the concentrated suspension. The reason could be that, in the concentrated suspension, the nanoparticles were more clustered owing to the much greater number of nanoparticles in the stabilised starting suspension. Such nanoparticle grouping is clearly visible in the FEG-ESEM observation (Fig. 12 bottom) of the agglomerated TiO_2 nanoparticles inside the 30 vol.% powder granules.

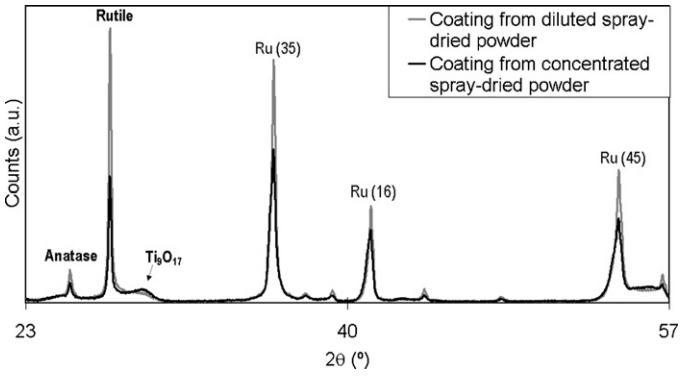

Fig. 13. XRD analysis of the nanostructured TiO_2 coatings produced from the spray-dried powder obtained from the diluted and the concentrated suspensions.

Finally, agglomerate apparent density (Table 5) of the granules obtained from the diluted and the concentrated suspensions was 1870 and 1620 kg/m^3, respectively. The Hausner ratio for both powders was <1.25, indicating good flowability. These characteristics make both powders appropriate for use as feedstock in the APS process.[12]

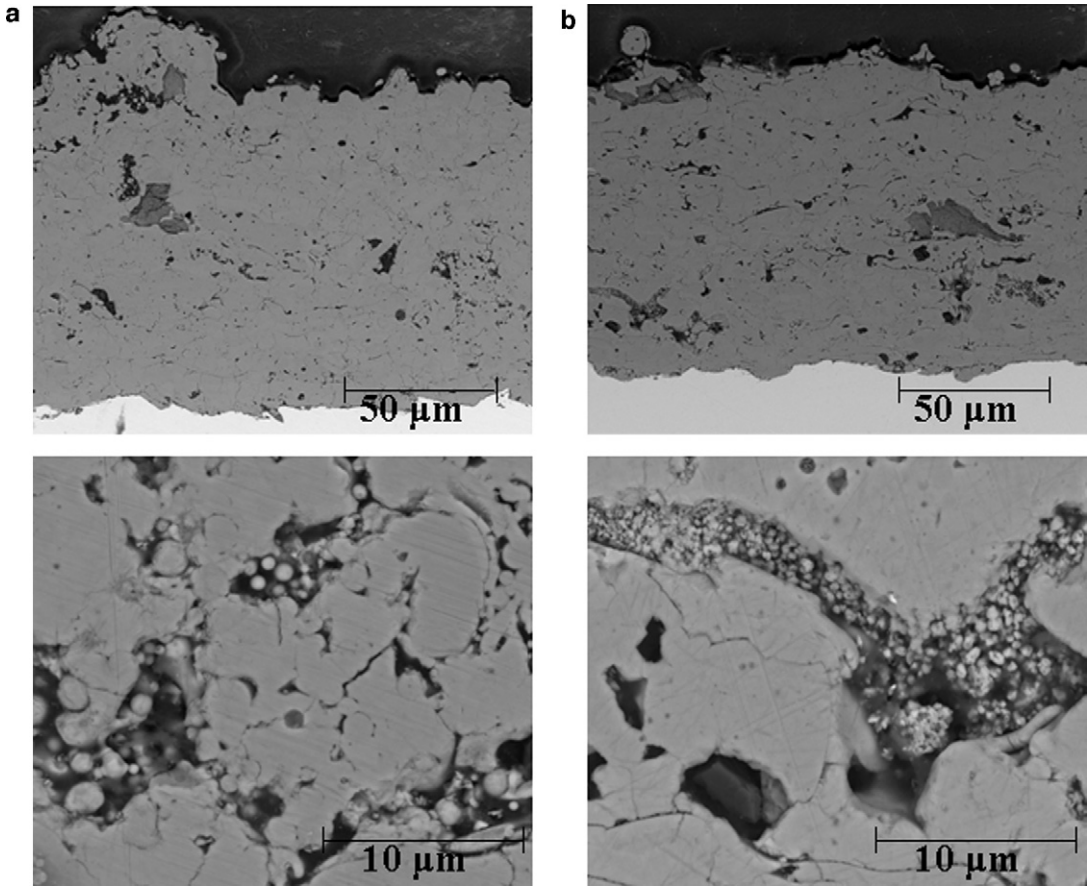

Fig. 14. FEG-ESEM micrographs of coatings produced from the spray-dried powder obtained from: a) diluted nanosuspensions and b) concentrated nanosuspensions.

3.5. Characterisation of the APS coatings

In the last step, the spray-dried granules obtained from the diluted commercial and the concentrated suspensions were deposited by APS, coatings being obtained of similar thickness and microstructure. These coatings were characterised by XRD, which indicated that both coatings contained mainly rutile and about 10% anatase (Fig. 13).

The FEG-ESEM micrographs of the microstructure (Fig. 14) show that the coatings consisted largely of dense areas (molten matrix). There were also some porous zones, pores, and partially molten areas containing fine nanometric and submicrometric grains made up of initial nanoparticles. These results are consistent with findings reported in previous studies, indicating that rutile is more prevalent than anatase in these fully melted regions.[31]

To increase the anatase fraction and, hence, photocatalytic activity, the melted regions need to be minimised by controlling plasma gas heat input in addition to feedstock characteristics. Recent research has also shown the influence of coating microstructure on photocatalysis performance.[32,33]

It should be noted that the purpose of the present research was to study the dispersion and stabilisation of titania nanopowder, as well as nanosuspension rheology, in order to obtain free-flowing spray-dried nanostructured granules for atmospheric plasma spraying. Further research is currently in progress to optimise plasma spraying conditions with different spray-dried feedstock in order to obtain coatings with improved microstructure and properties.

4. Conclusions

In this study, aqueous titania nanosuspensions were stabilised by means of an electrosteric mechanism. The effect of pH and sonication time was evaluated. Highly concentrated nanoparticle suspensions of TiO_2 were prepared from ~20-nm powders, using either distilled water or a commercial nanoparticle suspension as liquid medium. The solids content of the final suspension was 5 vol.% higher when the commercial nanosuspension was used.

The TiO_2 nanoparticles were reconstituted into plasma sprayable powders by spray drying. The resulting spray-dried powder properties made the powders appropriate for use as plasma spray feedstock. The use of concentrated suspensions for the reconstitution process enabled more regular, spherical spray-dried agglomerates with considerably higher porosity to be obtained, owing to the nanoparticle agglomerates inside the granule.

The reconstituted powders were deposited by atmospheric plasma spraying to obtain nanostructured coatings. All coatings displayed a bimodal microstructure, with partially molten agglomerates that retained the initial nanostructure of the feedstock surrounded by fully molten particles that acted as a binder. Further optimisation of the plasma spray parameters is needed in order to retain more nanostructured zones and to increase the anatase phase with a view to enhancing photocatalytic performance.

Acknowledgement

This study was supported by the Spanish Ministry of Science and Innovation (MAT2009-14144-C03-01, MAT2009-14369-C02-01, and PID-600200-2009-5).

References

1. Fujishima A, Zhang X. Titanium dioxide photocatalysis: present situation and future approaches. *CR Chim* 2006;**9**:750–60.
2. Ren LL, Zeng YP, Jiang DL. Preparation of porous TiO_2 sheets by aqueous tape casting and their photocatalytic activation. *Int J Appl Ceram Technol* 2008;**5**:505–12.
3. Chartier T, Merle D, Besson JL. Laminar ceramic composites. *J Eur Ceram Soc* 1995;**15**:101–7.
4. Lugscheider E, Bobzin K, Etzkorn A, Syrakas G, Siry CW. Graded EB-PVD-thermal barrier coatings produced by powder evaporation. *Adv Eng Mater* 2002;**4**:919–22.
5. Wang TM, Zheng SK, Hao WC, Wang C. Studies on photocatalytic activity and transmittance spectra of TiO_2 thin films prepared by r.f. magnetron sputtering method. *Surf Coat Technol* 2002;**155**:141–5.
6. Lima RS, Marple BR. Thermal spray coatings engineered from nanostructured ceramic agglomerated powders for structural, thermal barrier and biomedical applications: a review. *J Therm Spray Technol* 2007;**16**:40–63.
7. Morgiel J, Sánchez E, Grzonka J, Bannier E, Vicent M, Major L. The microstructure of WC–12%Co plasma sprayed coatings obtained from micro- and nano-powders. *Inzeria Materialowa* 2007;**28**:1–6.
8. Sánchez E, Cantavella V, Bannier E, Salvador MD, Klyastina E, Morgiel J, et al. Deposition of Al_2O_3–TiO_2 nanostructured powders by atmospheric plasma spraying. *J Therm Spray Technol* 2008;**17**:329–37.
9. Sánchez E, Bannier E, Vicent M, Moreno A, Salvador MD, Bonache V, et al. Characterization of nanostructured ceramic and cermet coatings deposited by plasma spraying. *Int J Appl Ceram Technol*, in press, DOI:10.1111/j.1744-7402.2010.02547.x.
10. Villanueva R, Gómez A, Burguete P, Beltrán A, Sapiña E, Vicent M, et al. Nanostructured alumina from freeze-dried precursors. *J Am Ceram Soc* 2011;**94**:237–44.
11. Vicent M, Sánchez E, Moreno R, Nieto MI. Study of Al_2O_3–TiO_2 granules obtained by freeze-drying process. In: Sánchez-Herencia AJ, Ferrari B, editors. *4th international conference on shaping of advanced ceramics*. 2009. p. S2–6.
12. Sánchez E, Vicent M, Moreno A, Salvador MD, Klyastina E, Bonache V, et al. Preparation and spray drying of nanoparticle Al_2O_3–TiO_2 suspensions to obtain nanostructured coatings by APS. *Surf Coat Technol* 2010;**205**:987–92.
13. Faure B, Lindeløv JS, Wahlberg M, Adkins N, Jackson P, Bergström L. Spray drying of TiO_2 nanoparticles into redispersible granules. *Powder Technol* 2010;**203**:384–8.
14. Tsung CK, Fan J, Zheng N, Shi Q, Forman AJ, Wang J, et al. A general route to diverse mesoporous metal oxide submicrospheres with highly crystalline frameworks. *Angew Chem Int Ed* 2008;**47**:8682–6.
15. Oveisi H, Suzuki N, Beitollahi A, Yamauchi Y. Aerosol-assisted fabrication of mesoporous titania spheres with crystallized anatase structures and investigation of their photocatalytic properties. *J Sol–Gel Sci Technol* 2010;**56**:212–8.
16. Yamauchi Y, Suzuki N, Gupta P, Sato K, Fukata N, Murakami M, et al. Aerosol-assisted synthesis of mesoporous organosilica microspheres with controlled organic contents. *Sci Technol Adv Mater* 2009;**10**:025005.
17. Norihiro S, Gupta P, Sukegawa H, Inomata K, Inoeu S, Yamauchi Y. Aerosol-assisted synthesis of thiol functionalized mesoporous silica spheres with Fe_3O_4 nanoparticles. *J Nanosci Nanotechnol* 2010;**10**:6612–7.
18. Kimura T, Kato K, Yamauchi Y. Temperature-controlled and aerosol-assisted synthesis of aluminium organophosphate spherical particles with uniform mesopores. *Chem Commun* 2009;**33**:4938–40.

19. Moreno R. The role of slip additives in tape-casting technology: part I. Solvents and dispersants. *Am Ceram Soc Bull* 1992;**71**:1521–30.
20. Amorín H, Santacruz I, Holc J, Thi MP, Kosec M, Moreno R, et al. Tape casting performance of ethanol slurries for processing textured PMN-PT ceramics from nanocrystalline powder. *J Am Ceram Soc* 2009;**92**:996–1001.
21. Negre F, Sánchez E. Advances in spray-dried pressing powder processes in tile manufacture. In: Henker VE, Onoda GY, Carty W, editors. *Science of whitewares*. Westerville: American Ceramic Society; 1996. p. 169–81.
22. Zainuddin MI, Tanaka S, Furushima R, Uematsu K. Correlation between slurry properties and structures and properties of granules. *J Eur Ceram Soc* 2010;**30**:3291–6.
23. Santacruz I, Annapoorani K, Binner J. Preparation of high solids content nano zirconia suspensions. *J Am Ceram Soc* 2008;**91**:398–405.
24. Santacruz I, Nieto MI, Binner J, Moreno R. Wet forming of concentrated nano $BaTiO_3$ suspensions. *J Eur Ceram Soc* 2009;**29**:881–6.
25. Fazio S, Guzmán J, Colomer MT, Salomoni A, Moreno R. Colloidal stability of nanosized titania aqueous suspensions. *J Eur Ceram Soc* 2008;**28**:2171–6.
26. Ohno T, Sarukawa K, Tokieda K, Matsumura M. Morphology of a TiO_2 photocatalyst (Degussa, P-25) consisting of anatase and rutile crystalline phases. *J Catal* 2001;**203**:82–6.
27. Vicent M, Sánchez E, Santacruz I, Moreno R. Dispersion of TiO_2 nanopowders to obtain homogeneous nanostructured granules by spray-drying. *J Eur Ceram Soc* 2011;**31**:1413–9.
28. Boschini F, Guillaume B, Rulmont A, Cloots R, Moreno R. Slip casting of barium zirconate aqueous concentrated suspensions. *J Eur Ceram Soc* 2006;**26**:1591–8.
29. Amorós JL, Blasco A, Enrique JE, Negre F. Características de polvos cerámicos para prensado [Characteristics of ceramic powders for pressing]. *Bol Soc Esp Ceram Vidr* 1987;**26**:31–7.
30. Bergström L. Rheological properties of concentrated, nonaqueous silicon nitride suspensions. *J Am Ceram Soc* 1996;**79**:3033–40.
31. Lee C, Choi H, Lee C, Kim H. Photocatalytic properties of nanostructured TiO_2 plasma sprayed coating. *Surf Coat Technol* 2003;**173**:192–200.
32. Podlesak H, Pawlowski L, Laureyns J, Jaworski T, Lampke T. Advanced microstructural study of suspension plasma sprayed titanium oxide coatings. *Surf Coat Technol* 2008;**202**:3723–31.
33. Kozerski S, Toma FL, Pawlowski L, Leupolt B, Latka L, Berger LM. Suspension plasma sprayed TiO_2 coatings using different injectors and their photocatalytic properties. *Surf Coat Technol* 2010;**205**:980–6.